RevMexAA (Serie de Conferencias), **6**, 96–98 (1997)

PHYSICAL DIAGNOSTICS OF EMISSION-LINE GALAXIES IN DEEP SURVEYS

Cláudia S. Rola[1,2], Elena Terlevich[1], and Roberto Terlevich[2]

RESUMEN

Se presentan diagramas de diagnóstico para clasificar galaxias con líneas de emisión, en particular aquellas encontradas en relevamientos con desplazamientos al rojo intermedios, usando sólo las líneas de [O II] y Hβ, así como el contínuo adyacente.

ABSTRACT

We present new diagnostic diagrams to identify the nature of emission-line galaxies, specially useful for deep surveys as the calibration is based in a minimum of observational data and reddening corrections and flux calibration are not essential. The new diagrams use only the [O II]λ3727,3729 and H$_\beta$ emission-lines and the adjacent continuum.

Key words: **GALAXIES: GENERAL – GALAXIES: ISM — LINE: FORMATION**

1. INTRODUCTION

Several redshift surveys (e.g., Broadhurst, Ellis, & Shanks 1988; Lavery & Henry 1988; Colless et al. 1990) have produced an extensive data-base of spectroscopy of galaxies at moderate redshifts ($z \approx 0 - 0.7$); still, very little is known about the nature of the emission-line galaxies (ELGs).

Nearby ELGs are generally classified by diagnostic diagrams, using emission line intensity ratios: [O I]λ6300 Å, [O II]$\lambda\lambda$3727, 3729 Å, [O III]λ5007 Å, [N II]λ6584 Å, [S II]$\lambda\lambda$6717, 6730 Å, Hα and Hβ (see Baldwin, Philips, & Terlevich 1981; Veilleux & Osterbrock 1987). At z beyond ≈ 0.3 most of the strong emission-lines move out of the optical spectral range. The last ones remaining are Hβ, observable up to $z \approx 0.75$, and [O II]λ3727 Å up to $z \approx 1.3$. This renders the existent diagnostic methods useless for distant objects found in optical redshift surveys where most of the ELGs are hence classified using the [O II]λ3727 Å emission-line, namely its equivalent width, to avoid flux calibration. Recent results from the Canada-France Redshift Survey (see Tresse et al. 1996) suggest that in deep surveys the probability that an observed ELG is an active galaxy could be higher than expected from local surveys. Therefore, it is important to find new diagnostic methods that are appropriate to deep surveys. They should require a minimum of spectral coverage preferably in the blue.

For this purpose, we considered a statistically significant (though not complete) local sample of ELGs: H II galaxies, Seyfert 2 and LINERs, mainly from the Terlevich et al. (1991) spectrophotometric catalogue of H II galaxies where some active galaxies were also observed. The sample was then classified, and the classification transferred to new diagrams using only the few emission-lines that are usually available to redshift surveys, and continuum information. We selected a set of new diagrams which quite distinctly separate H II from active galaxies.

2. CLASSIFICATION OF THE DATA SAMPLE

The classification of the sample in active and H II galaxies was based on four standard diagnostic diagrams, using reddening corrected intensity line ratios, combined with a grid of photoionisation models.

[1]Institute of Astronomy, University of Cambridge, UK.

[2]Royal Greenwich Observatory, Cambridge, UK.

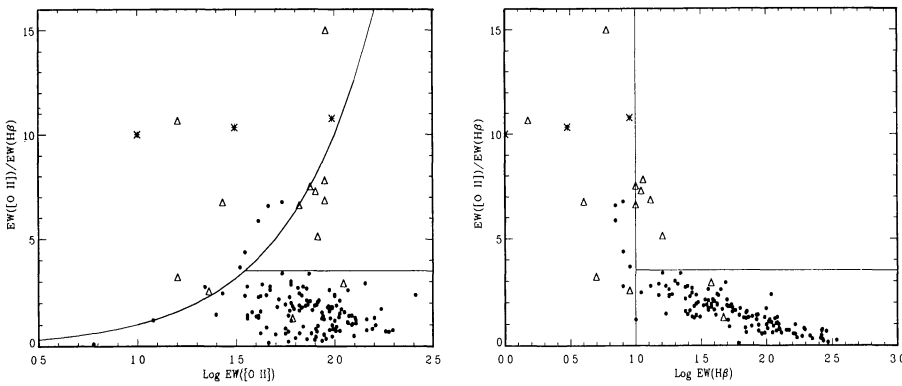

Fig. 1. EW([O II])/EW(Hβ) vs. EW([O II]) (left) and EW(Hβ) (right). The left and right upper sections define the region where active galaxies lie while the H II galaxies region is the bottom right one.

2.1. Photoionisation models

The boundary between H II and active galaxies in the diagnostic diagrams above mentioned was first determined theoretically using an extensive grid of steady-state spherically symmetric H II region models (Rola 1995). This grid allows us to obtain the upper limit for the location of nebulae photoionised by OB stars in diagnostic diagrams: ELGs above this limit are surely active galaxies (Seyfert 2s or LINERs). In order to determine the loci of H II regions in the diagrams, we have considered wide ranges for their typical physical parameters.

It is rather difficult to define the exact boundary separating H II from active galaxies in diagnostic diagrams. This is mainly due to uncertainties in the stellar atmospheres spectra, in the actual value of the upper limit for the stellar effective temperature of the hottest stars, and in the values of atomic coefficients used in the photoionisation models. Actually, the limit should be situated somewhere between the two theoretical separation curves defined by the models at $T_{\rm eff} = 50\,000$ K and $T_{\rm eff} = 60\,000$ K. Therefore, we have determined the nature of our sample ELGs using both boundaries and if a galaxy appeared as H II and active in an equivalent number of diagrams, its final classification was kept undetermined. Seyfert 2s were separated from LINERs in a second step. Based on observational data from the literature (e.g., Veilleux & Osterbrock 1987; Fillipenko & Terlevich 1992; Coziol 1996), we classified galaxies with log [O III]λ5007/H$_\beta$ < 0.5 as LINERs. The galaxies which predominantly fell between both separation curves in the diagnostic diagrams, called *transition* galaxies, were not considered in our final statistical analysis.

Out of 231 ELGs from which 9 are transition objects, we classified 131 as H II galaxies, 14 as Seyfert 2s and 5 as LINERs. 72 objects remained unclassified, either due to lack of data or to ambiguity in the classification.

3. NEW DIAGNOSTIC DIAGRAMS

It is important to be able to determine the nature of redshifted ELGs independently of reddening and using a minimum number of —preferably blue— emission-lines as the red ones would have redshifted out of the observed window. We based our new diagnostic diagrams on [O II]λ3727 and Hβ, both lines being generally present in the optical range up to $z \approx 0.75$. We decided to use mainly equivalent widths (which are essentially reddening independent). We have also used the information from the adjacent continuum.

In the diagrams that follow, *dot* symbols represent *H II galaxies*, *triangles Seyfert 2* and *asterisks LINERs*. In Figure 1 we plotted EW([O II]λ3727)/EW(Hβ) against EW([O II]) and against EW(Hβ). The lines drawn in each diagram define three zones. The horizontal lines were defined by inspection of the distribution of the EW([O II]λ3727)/EW(Hβ) ratio. It is found that about 79% of all the active galaxies in the data sample (against 4% of the H II galaxies) are located above 3.5. The curve and vertical lines in the diagrams are based in the analysis of the data, where we have found that an EW(Hβ) of 10 A is a good upper limit to separate active from H II galaxies (given that only a few H II galaxies lie below this limit).

Thus, the combination of these two limits leads to the following separation zones in both diagrams of Figure 1. The first one corresponds to the lower right region (henceforth called *H II region*), where most of the H II galaxies and only a few active ones fall. It is limited upwards by the curve at EW([O II]λ3727)/EW(Hβ) =

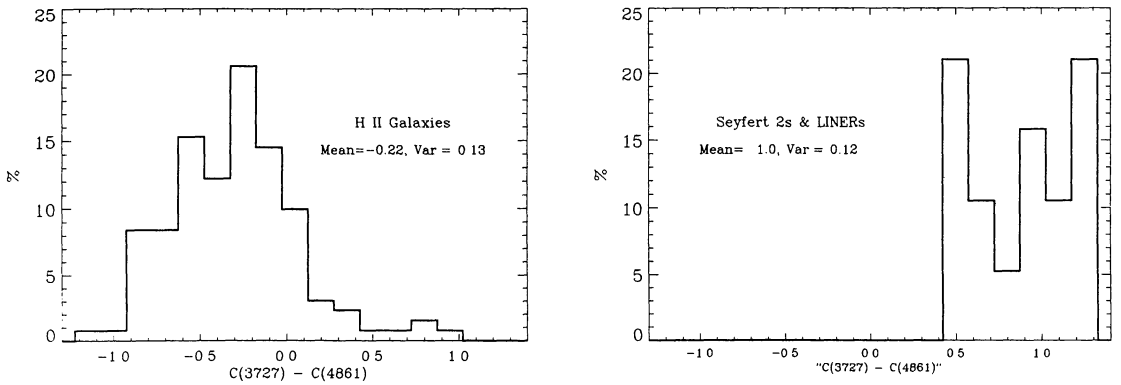

Fig. 2. Distribution of the $C_{3727} - C_{4861}$ colour index for H II galaxies (left diagram) and for AGNs (right diagram). The percentages are relative to the total number of galaxies of each type.

3.5 and leftwards by the curve EW(Hβ) = 10 Å. About 87% of all H II galaxies in our sample are located here against 15% of all Seyfert 2's and 0% of all LINERs (which represents about 12% of all our active galaxies). The second one (hereafter called *AGN region*) corresponds to the opposite region, where EW([O II]λ3727)/EW(Hβ) $\geq$3.5 and the EW(Hβ) > 10 Å *plus* all the region where EW(Hβ) <10 Å. About 85% of all Seyfert 2s and 100% of all LINERs in our sample are located here (about 88% of all our active galaxies) against 13% of all H II galaxies. These percentages, relative to each type of galaxy, represent the probability for a given type of object to fall in a given region of the diagram. From them, we can determine the probability that an ELG which falls in a given region is either an active (Seyfert 2 or LINER) or an H II galaxy. This can be calculated if we consider that, for each region, the sum of the probabilities, i.e., the probability of being an active galaxy ($\mathrm{Prob_{region}(AGN)}$) *plus* the probability of being an H II galaxy ($\mathrm{Prob_{region}(H\ II)}$) is equal to 1. This leads to determine that in the AGN region, $\mathrm{Prob_{AGN}(AGN)} \approx 95\%$ and $\mathrm{Prob_{AGN}(H\ II)} \approx 5\%$, while in the H II region, $\mathrm{Prob_{H\ II}(AGN)} \approx 10\%$ and $\mathrm{Prob_{H\ II}(H\ II)} \approx 90\%$. This implies that Figure 1 diagrams are very efficient in separating Seyfert 2s and LINERs from H II galaxies.

We have defined a continuum colour index, given by $C_{3727} - C_{4861} = 2.5 \times \log_{10}\left(\frac{C_{H\beta}}{C_{[OII]\lambda 3727}}\right)$, (where C_{3727} and C_{4861} represent the intensity of the continuum under the [O II]λ3727 and Hβ emission-lines, respectively). Higher $C_{3727} - C_{4861}$ values correspond to a redder continuum. The histograms in Figure 2 show that the mean and variance of the distribution of this colour index is about 1.0 and 0.12, respectively, for active galaxies (Seyfert 2s and Liners) and about −0.22 and 0.13, respectively for H II galaxies.. Active galaxies tend to have higher values of $C_{3727} - C_{4861}$ than H II galaxies because their spectra are generally redder. This is due to the dominant stellar populations in these objects: old stars, like red giants, contribute significantly to the active galaxies continuum while young OB stars are the main contributors to the continuum of H II galaxies. The $C_{3727} - C_{4861}$ colour index can then be very useful in separating both types of objects.

Figures 1 and 2 provide a strong and valuable diagnostic of the nature of ELG's which seems not to be very much affected by galaxy evolution, at least up to intermediate redshifts as fully discussed in Rola, Terlevich, & Terlevich (in preparation).

REFERENCES

Baldwin, J., Philips, M., & Terlevich, R. 1981, PASP, 93, 5
Broadhurst, T., Ellis, R. S., & Shanks, T. 1988, MNRAS, 235, 827
Colless, M., Ellis, R. S., Taylor, K., & Hook, R. N. 1990, MNRAS, 244, 408
Coziol, R. 1996, A&A, 309, 345
Lavery, R., & Henry, J. P. 1988, ApJ, 330, 596
Fillipenko, A., & Terlevich, R., 1992, ApJ, 397, 79
Rola, C. S. 1995, Ph.D. thesis, Université de Paris VII, France
Terlevich, R., Melnick, J., Masegosa, J., Moles, M., & Copetti, M. 1991, A&AS, 91, 285
Tresse, L., Rola, C. S., Hammer, F., Stasiǹska, G., Le Fèvre, O., Lilly, S., & Crampton, D. 1996, MNRAS, 281, 847
Veilleux, S., & Osterbrock, D. 1987, ApJS, 63, 295